THE JOURNAL OF BIOLOGICAL CHEMISTRY VOL. 289, NO. 47, pp. 32593–32603, November 21, 2014
Published in the U.S.A.

Interaction between the Pentose Phosphate Pathway and Gluconeogenesis from Glycerol in the Liver*[S]

Received for publication, April 30, 2014, and in revised form, October 2, 2014 Published, JBC Papers in Press, October 6, 2014, DOI 10.1074/jbc.M114.577692

Eunsook S. Jin[‡§1], **A. Dean Sherry**[‡¶‖], **and Craig R. Malloy**[‡§¶**]

From the [‡]*Advanced Imaging Research Center and Departments of* [§]*Internal Medicine and* [¶]*Radiology, University of Texas Southwestern Medical Center, Dallas, Texas 75390, the* [‖]*Department of Chemistry, University of Texas at Dallas, Richardson, Texas 75080, and the* [**]*Veterans Affairs North Texas Health Care System, Dallas, Texas 75216*

Background: Hepatic pentose phosphate pathway activity is difficult to monitor *in vivo*.
Results: Hepatic pentose phosphate pathway results in different ratios of doubly labeled glucose isotopomers after administration of [U-$^{13}C_3$]glycerol.
Conclusion: [1,2-$^{13}C_2$]glucose produced by the hepatic pentose phosphate pathway is quantified.
Significance: A simple method is presented to detect the activity of hepatic pentose phosphate pathway *in vivo* from analysis of plasma glucose.

After exposure to [U-$^{13}C_3$]glycerol, the liver produces primarily [1,2,3-$^{13}C_3$]- and [4,5,6-$^{13}C_3$]glucose in equal proportions through gluconeogenesis from the level of trioses. Other ^{13}C-labeling patterns occur as a consequence of alternative pathways for glucose production. The pentose phosphate pathway (PPP), metabolism in the citric acid cycle, incomplete equilibration by triose phosphate isomerase, or the transaldolase reaction all interact to produce complex ^{13}C-labeling patterns in exported glucose. Here, we investigated ^{13}C labeling in plasma glucose in rats given [U-$^{13}C_3$]glycerol under various nutritional conditions. Blood was drawn at multiple time points to extract glucose for NMR analysis. Because the transaldolase reaction and incomplete equilibrium by triose phosphate isomerase cannot break a ^{13}C-^{13}C bond within the trioses contributing to glucose, the appearance of [1,2-$^{13}C_2$]-, [2,3-$^{13}C_2$]-, [5,6-$^{13}C_2$]-, and [4,5-$^{13}C_2$]glucose provides direct evidence for metabolism of glycerol in the citric acid cycle or the PPP but not an influence of either triose phosphate isomerase or the transaldolase reaction. In all animals, [1,2-$^{13}C_2$]glucose/[2,3-$^{13}C_2$]glucose was significantly greater than [5,6-$^{13}C_2$]glucose/[4,5-$^{13}C_2$]glucose, a relationship that can only arise from gluconeogenesis followed by passage of substrates through the PPP. In summary, the hepatic PPP *in vivo* can be detected by ^{13}C distribution in blood glucose after [U-$^{13}C_3$]glycerol administration.

Gluconeogenesis has been studied extensively after administration of carbon-labeled glycerol, pyruvate, or equivalent molecules with the goal of understanding the carbon sources and control of hepatic glucose production. The distribution of a carbon isotope in glucose released from liver *in vivo* after administration of a labeled gluconeogenic substrate is determined by relative fluxes through four metabolic pathways or individual enzymes. The triose phosphate isomerase (TPI)[2] reaction influences equilibration of tracer between carbons 1–3 and carbons 4–6 of glucose. Essentially complete equilibration has been assumed in studies with hydrogen and carbon tracers (1–3) or confirmed experimentally in some preparations (4–5). However, others find that equilibration is incomplete (6–10). A second pathway relevant to tracers originating in both pyruvate and glycerol (11) is metabolism in the citric acid cycle (CAC) with rearrangement and dilution of the carbon tracer, followed by gluconeogenesis from phosphoenolpyruvate (PEP). The activity of transaldolase is a third factor that may influence carbon labeling in glucose derived from trioses. Transaldolase catalyzes removal of a three-carbon unit from sedoheptulose 7-phosphate in the non-oxidative arm of the pentose phosphate pathway (PPP). The three-carbon unit can then condense with glyceraldehyde 3-phosphate (GA3P) to yield fructose 6-phosphate (F6P) and erythrose 4-phosphate. The transaldolase reaction also directly exchanges carbons 4–6 of F6P with GA3P (12–17). The fourth relevant pathway involves possible redistribution of carbon tracers in the oxidative arm of the PPP. Here, carbon 1 of glucose 6-phosphate (G6P) is lost to generate a pentose that is either utilized in nucleotide synthesis or cycled back into F6P or trioses. The PPP rearranges the order of carbons 1–3 of glucose, but it does not alter the order of carbons 4–6 of glucose. The details of this rearrangement were established previously (18–20).

In previous studies of gluconeogenesis from either ^{13}C- or ^{14}C-labeled precursors, the distribution of the tracer was measured in glucose, and metabolic models of varying complexity were used to assess the relative activity of these pathways. Because of the relative simplicity of working with stable isotopes, ^{13}C-labeled precursors have been emphasized recently. If all four pathways are included in the analysis of ^{13}C distribution

* This work was supported by National Institutes of Health Grants DK078933 and DK099289 (to E. S. J.), RR 002584 and EB 015908 (to C. R. M.), and HL-34557 (to A. D. S.).
[S] This article contains supplemental Fig. 1.
[1] To whom correspondence should be addressed: Advanced Imaging Research Center, 5323 Harry Hines Blvd., Dallas, TX 75390-8568. Tel.: 214-645-2725; Fax: 214-645-2744; E-mail: eunsook.jin@utsouthwestern.edu.

[2] The abbreviations used are: TPI, triose phosphate isomerase; CAC, citric acid cycle; DHAP, dihydroxyacetone phosphate; F6P, fructose 6-phosphate; GA3P, D-glyceraldehyde 3-phosphate; GNG, gluconeogenesis; G6P, glucose 6-phosphate; MAG, monoacetone glucose; PEP, phosphoenolpyruvate; PPP, pentose phosphate pathway.

in glucose, interpretation of experimental data is challenging because some pathways have equivalent effects on ^{13}C labeling in glucose. For example, in the presence of ^{13}C-labeled lactate, selective enrichment in carbons 4–6 relative to carbons 1–3 of glucose will occur as a consequence of either the transaldolase activity or incomplete equilibration by TPI. Complex labeling patterns in carbons 1–3 can also occur due to the PPP or metabolism in the CAC. Although these four pathways certainly have interacting effects on ^{13}C labeling in glucose, failure to establish equilibrium at the level of TPI or the transaldolase reaction cannot influence the ^{13}C distribution within the trioses contributing to glucose, allowing some simplification in interpretation. Recently, we examined the sources of the glycerol moiety of hepatic acylglycerols in animals given a mixture of glucose, glycerol, and lactate (11). Using a similar approach in the current study, we found surprising ^{13}C asymmetry between carbons 1–3 and carbons 4–6 of plasma glucose after administration of [U-$^{13}C_3$]glycerol which was not observed in animals given [U-$^{13}C_3$]lactate. Here, we examined the mechanism of this discrepancy in detail and presented a novel approach to estimate activity of the hepatic PPP *in vivo* based on ^{13}C labeling in blood glucose after [U-$^{13}C_3$]glycerol administration.

MATERIALS AND METHODS

Protocol—The study was approved by the Institutional Animal Care and Use Committee at the University of Texas Southwestern Medical Center. Male Sprague-Dawley rats (346 ± 3g) were handled as described previously (11). Briefly, fed or 24-hour fasted rats received an intraperitoneal injection of (*a*) a mixture of glucose (2 g/kg), lactate (0.5 g/kg), and [U-$^{13}C_3$]-glycerol (0.5 g/kg) or (*b*) a mixture of glucose, [U-$^{13}C_3$]lactate and glycerol. After 3 h of mixture administration, blood was drawn from the inferior vena cava under isoflurane anesthesia.

Other groups of rats were fasted for 24 h with free access to water. All animals received an intraperitoneal injection of [U-$^{13}C_3$]glycerol (50%) based on body weight (25 mg/kg, 50 mg/kg, 100 mg/kg, or 500 mg/kg). After waiting for 30, 60, 120, or 180 min, blood was drawn under anesthesia and was further processed for NMR analysis. This experiment was repeated with a group of fed rats using 100 mg/kg [U-$^{13}C_3$]glycerol (50%), and blood was sampled after 60 min.

Sample Processing for NMR Analysis—Blood was immediately centrifuged, and plasma supernatant was deproteinized by adding perchloric acid to a final concentration of 7%. After neutralization with KOH and centrifugation, the supernatant was lyophilized. The dried residue was applied to an ion-exchange column containing 15 ml of cation- and 15 ml of anion-exchange resin with water as eluent to purify glucose, and it was lyophilized. To convert glucose into monoacetone glucose (MAG), dried glucose was suspended in 3.0 ml of acetone containing 120 μl of concentrated sulfuric acid. The mixture was stirred for 4 h at room temperature to yield diacetone glucose. After adding 3 ml of water, pH was adjusted to 2.0 by dropwise addition of 1.5 M Na_2CO_3. The mixture was stirred for 24 h at room temperature to convert diacetone glucose into MAG. The pH was then further increased to ~8.0 by addition of Na_2CO_3. Acetone was evaporated under vacuum, and the sample was lyophilized. MAG was extracted into 5 ml of hot ethyl acetate (5×), and ethyl acetate was removed by vacuum evaporation. The resulting MAG was further purified by passage through a 3-ml DSC-18 cartridge, using 5% acetonitrile as eluant. The effluent was lyophilized and stored dry before NMR analysis.

NMR Spectroscopy—All NMR spectra were collected using a Varian INOVA 14.1-T spectrometer (Agilent, Santa Clara, CA) equipped with a 3-mm broadband probe with the observe coil tuned to ^{13}C (150 MHz). MAG was resuspended in 160 μl of deuterated acetonitrile and 10 μl of water. After shimming to optimize the homogeneity of the magnetic field, ^{13}C NMR spectra were collected using a 52° observe pulse (6.06 μs), 60992 data points collected over a sweep-width of 20,330 Hz, and a 1.5-s acquisition time with 1.5-s interpulse delay at 25 °C. Proton decoupling was performed using a standard WALTZ-16 pulse sequence. Typically ~25,000 scans were averaged, requiring ~21 h. All NMR spectra were analyzed using ACD/Labs PC-based NMR spectral analysis program (Advanced Chemistry Development, Inc., Toronto, Canada).

^{13}C Asymmetry in Glucose Isotopomers Released from Liver Supplied with [U-$^{13}C_3$]Glycerol—After exposure to [U-$^{13}C_3$]-glycerol, four pathways will influence the distribution of ^{13}C in glucose: the extent of equilibration at TPI, the PPP, metabolism of glycerol in the CAC followed by gluconeogenesis, and the transaldolase reaction. In gluconeogenesis, carbons 1–3 of glucose (the "top" half) are derived from dihydroxyacetone phosphate (DHAP), whereas carbons 4–6 (the "bottom" half) are derived from GA3P (see Fig. 1*A*). After exposure to [U-$^{13}C_3$]glycerol, the liver produces primarily [1,2,3-$^{13}C_3$]glucose and [4,5,6-$^{13}C_3$]glucose after equilibration of DHAP and GA3P through TPI. [U-$^{13}C_6$]glucose is also produced, but it will not be considered further for simplicity because it is trivial in the current study. Other labeling patterns cannot occur, and equal ^{13}C labeling is expected between carbons 1–3 and carbons 4–6 of glucose ([1,2,3-$^{13}C_3$] = [4,5,6-$^{13}C_3$]; see Fig. 1*B*) if the following conditions are met: 1) glycerol is not metabolized in the CAC prior to entering gluconeogenesis, 2) there is complete equilibration of DHAP and GA3P by TPI, 3) transaldolase is inactive, and 4) the PPP is inactive. If all four conditions are met, then the ^{13}C NMR spectrum of glucose is not particularly interesting. If, however, any of these four conditions do not apply, then other isotopomers of glucose will be evident and the NMR readout becomes more informative.

Metabolism of [U-$^{13}C_3$]glycerol in the CAC enables generation of doubly labeled glucose isotopomers (see Fig. 1*C*). [U-$^{13}C_3$]pyruvate produced from [U-$^{13}C_3$]glycerol can enter the CAC via pyruvate carboxylase or pyruvate dehydrogenase. After ^{13}C scrambling in the cycle, ^{13}C-labeled oxaloacetate exits the cycle via PEP carboxykinase to yield four possible isotopomers: [2,3-$^{13}C_2$]PEP, [1,2-$^{13}C_2$]PEP, [U-$^{13}C_3$]PEP, and [3-$^{13}C_1$]PEP (11). The first two isotopomers reflect ^{13}C decarboxylation and are the important ones emphasized here. Any [U-$^{13}C_3$]PEP generated from a CAC intermediate cannot be distinguished from the original [U-$^{13}C_3$]glycerol, whereas the singly-labeled isotopomer ([3-$^{13}C_1$]PEP) cannot be distinguished from natural abundance ^{13}C by NMR spectroscopy. [2,3-$^{13}C_2$]PEP and [1,2-$^{13}C_2$]PEP are converted to [2,3-$^{13}C_2$]GA3P and [1,2-$^{13}C_2$]GA3P, respectively, via reversal of glycolysis and, depending on the extent of equilibration at TPI

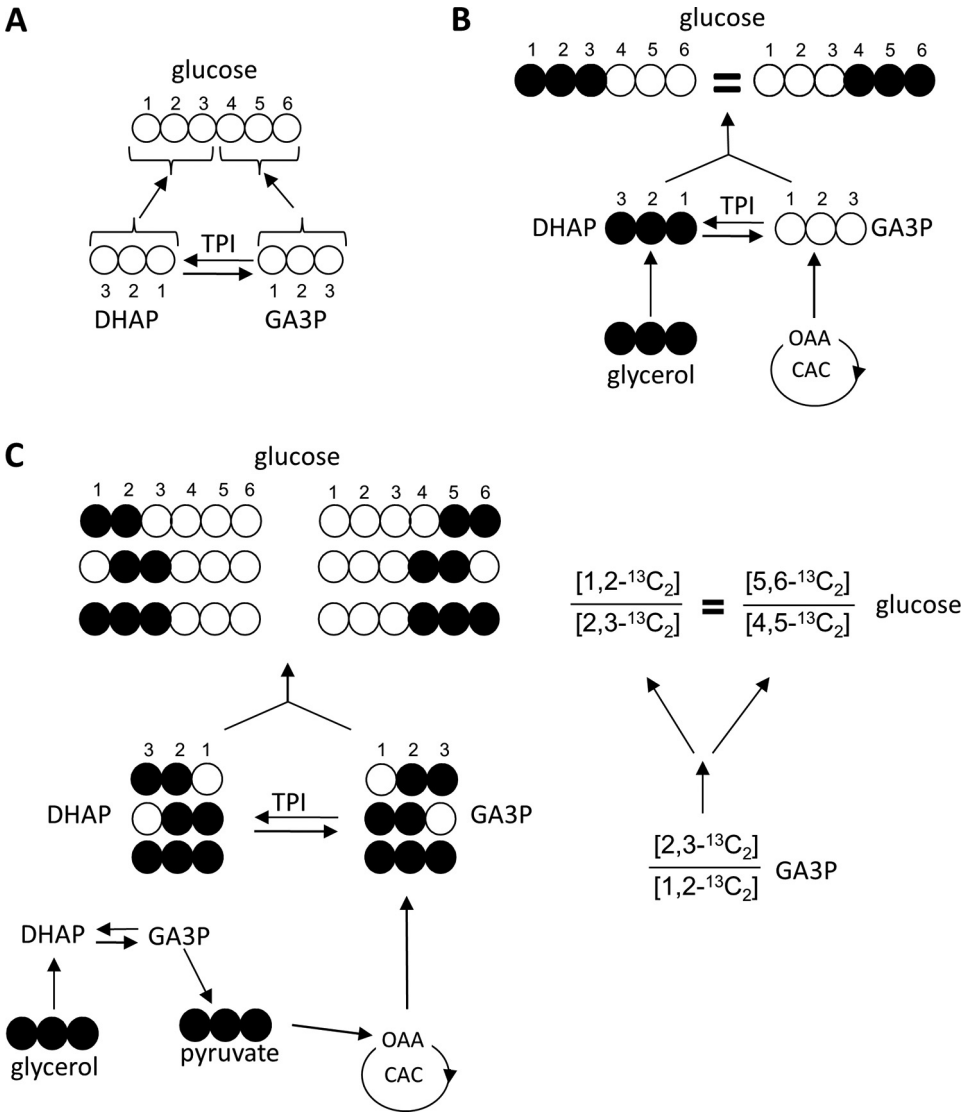

FIGURE 1. **^{13}C symmetry between the top and bottom half of glucose from liver supplied with [U-$^{13}C_3$]glycerol.** DHAP and GA3P condense during gluconeogenesis. Carbons 1–3 of glucose originate from DHAP, whereas carbons 4–6 originate from GA3P (*A*). The liver would produce equal amounts of [1,2,3-$^{13}C_3$]glucose and [4,5,6-$^{13}C_3$]glucose from [U-$^{13}C_3$]glycerol if there is complete equilibrium at the level of TPI, no PPP, and no transaldolase activity (*B*). If a small portion of [U-$^{13}C_3$]glycerol enters the CAC prior to gluconeogenesis, a set of GA3P isotopomers ([2,3-$^{13}C_2$]-, [1,2-$^{13}C_2$]-, [U-$^{13}C_3$]GA3P) are produced, which are common intermediates for both top and bottom half carbons of glucose. Consequently, there would be equal in the ratios of [1,2-$^{13}C_2$]/[2,3-$^{13}C_3$] and [5,6-$^{13}C_2$]/[4,5-$^{13}C_2$] if the PPP is not active (*C*). Transaldolase activity or disequilibrium at the level of TPI does not influence the relative amount of [1,2-$^{13}C_2$]- and [2,3-$^{13}C_2$]glucose (or the relative amount of [5,6-$^{13}C_2$]- and [4,5-$^{13}C_2$]glucose) because neither pathway disrupts the information encoded by the ^{13}C distribution within the three-carbon unit. *OAA*, oxaloacetate; *open circle*, ^{12}C; *filled circle*, ^{13}C.

or rearrangements due to transaldolase, the eventual contribution to carbons 1–3 or 4–6 of glucose can vary considerably. However, the relative amounts of [2,3-$^{13}C_2$]GA3P and [1,2-$^{13}C_2$]GA3P cannot be altered by either TPI or transaldolase activity (Fig. 1*C*).

Disequilibrium at the level of TPI could, however, result in a difference in the extent of ^{13}C labeling in the top half *versus* bottom half of glucose. After [U-$^{13}C_3$]glycerol phosphorylation, it is converted to [U-$^{13}C_3$]DHAP first before [U-$^{13}C_3$]-GA3P through TPI. Thus, in the absence of other influences, any disequilibrium at the level of TPI would result in [1,2,3-$^{13}C_3$]glucose > [4,5,6-$^{13}C_3$]glucose (Fig. 2*A*).

The third pathway to consider individually is the effect of transaldolase. In contrast to the effects of disequilibrium at the level of TPI, the opposite glucose asymmetry ([1,2,3-$^{13}C_3$] < [4,5,6-$^{13}C_3$]) would result from any transaldolase activity. Transaldolase catalyzes removal of a three-carbon unit from the non-phosphorylated end of sedoheptulose 7-phosphate, and this three-carbon unit can then condense with [U-$^{13}C_3$]-GA3P that might be present to yield [4,5,6-$^{13}C_3$]F6P and erythrose 4-phosphate. This [4,5,6-$^{13}C_3$]F6P would be readily converted to [4,5,6-$^{13}C_3$]G6P and subsequently [4,5,6-$^{13}C_3$]glucose (Fig. 2*B*). Ljungdahl *et al.* (14) demonstrated that isolated transaldolase can exchange carbons 4–6 of F6P with GA3P even in the absence of other enzymes or intermediates of PPP. The capacity to detect transaldolase activity as described by Ljungdahl *et al.* (14) requires incomplete equilibration at the level of TPI. If the ^{13}C-labeling pattern in DHAP and GA3P are identical, then transaldoalse activity cannot influence the distribution of ^{13}C in glucose synthesized from this triose pool.

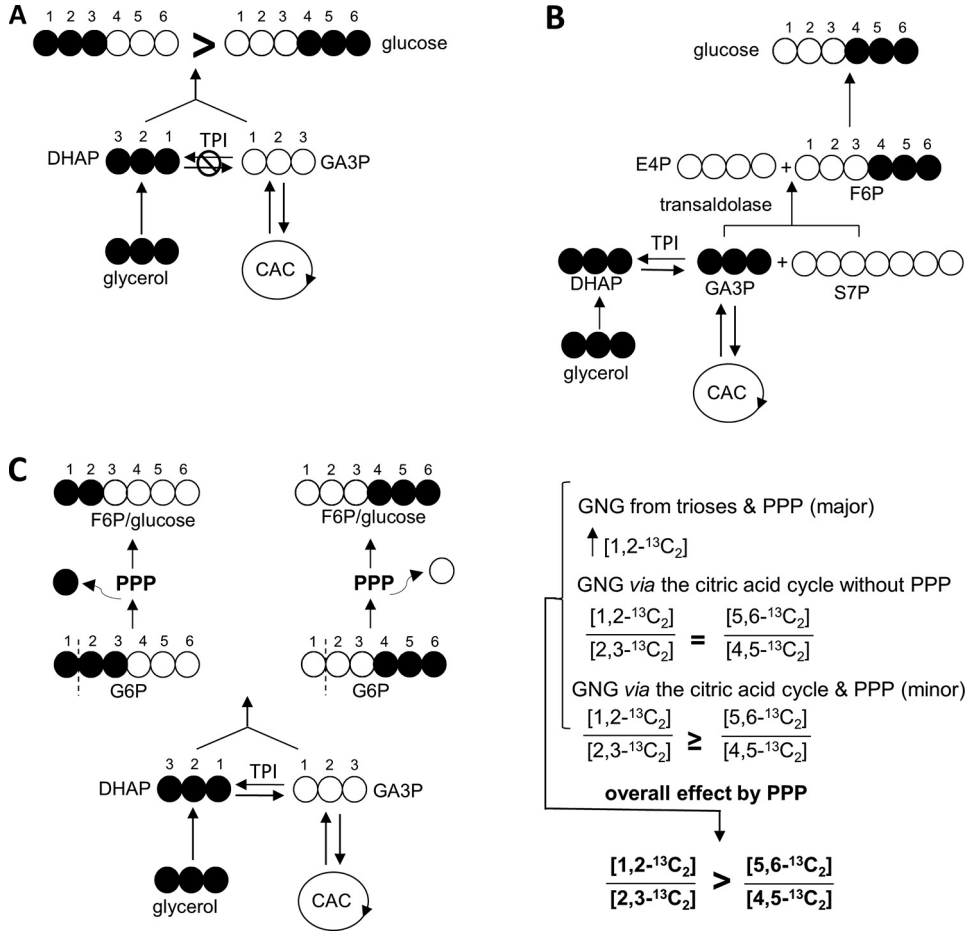

FIGURE 2. **^{13}C Asymmetry between the top and bottom half of glucose from the liver supplied with [U-$^{13}C_3$]glycerol.** Any lack of complete equilibrium at the level of TPI causes [1,2,3-$^{13}C_3$]glucose > [4,5,6-$^{13}C_3$]glucose because [U-$^{13}C_3$]glycerol was converted to [U-$^{13}C_3$]DHAP first before [U-$^{13}C_3$]GA3P through TPI (*A*). After [U-$^{13}C_3$]glycerol phosphorylation, [U-$^{13}C_3$]GA3P was produced through TPI activity. Transaldolase reaction between [U-$^{13}C_3$]GA3P and sedoheptulose 7-phosphate (*S7P*) produces [4,5,6-$^{13}C_3$]F6P and erythrose 4-phosphate, and consequently [4,5,6-$^{13}C_3$]glucose (*B*). After [U-$^{13}C_3$]glycerol administration, [1,2,3-$^{13}C_3$]- and [4,5,6-$^{13}C_3$]hexose are the main isotopomers through gluconeogenesis from the level of trioses. The entry of [1,2,3-$^{13}C_3$]G6P into the PPP produces primarily [1,2-$^{13}C_2$]F6P, and consequently [1,2-$^{13}C_2$]glucose, but the PPP does not change the labeling patterns in bottom half carbons of the hexose (*C*). The entry of [U-$^{13}C_3$]glycerol into the CAC prior to gluconeogenesis would result in [1,2-$^{13}C_2$]/[2,3-$^{13}C_3$] = [5,6-$^{13}C_2$]/[4,5-$^{13}C_2$] in glucose if the PPP is not active, but [1,2-$^{13}C_2$]/[2,3-$^{13}C_2$] ≥ [5,6-$^{13}C_2$]/[4,5-$^{13}C_2$] if the PPP is active. Thus, the difference of [1,2-$^{13}C_2$]/[2,3-$^{13}C_2$] and [5,6-$^{13}C_2$]/[4,5-$^{13}C_2$] in glucose is sensitive to the hepatic PPP activity. *E4P*, erythrose 4-phosphate; *GNG*, gluconeogenesis.

However, if TPI is not fully equilibrated or if this exchange between F6P and [U-$^{13}C_3$]GA3P should occur in the liver of whole animals where unlabeled glucose is present, then the combined process would result in preferential labeling of the carbons 4–6 of glucose from [U-$^{13}C_3$]glycerol.

The fourth factor that may influence the distribution of ^{13}C in glucose is the PPP. Although the complete PPP seems rather complicated (Fig. 3), the consequence of this pathway is relatively easily described. In the liver supplied with [U-$^{13}C_3$]-glycerol, [1,2,3-$^{13}C_3$]- and [4,5,6-$^{13}C_3$]hexose are the main isotopomers. Passage of [1,2,3-$^{13}C_3$]G6P through the PPP largely produces [1,2-$^{13}C_2$]F6P = [1,2-$^{13}C_2$]glucose, whereas the labeling pattern of [4,5,6-$^{13}C_3$]G6P after passage through the PPP remains unchanged (Fig. 2*C*). Thus, the presence of excess [1,2-$^{13}C_2$]glucose signifies an active PPP.

The next step is to consider the combined effects of these pathways. As noted above, transaldolase or the extent of disequilibrium at the level of TPI is to cause asymmetric distribution of an intact three-carbon unit into either the top or bottom half of glucose. However, the information encoded by the ^{13}C distribution within the three-carbon unit is not disrupted because carbon-carbon bonds are not broken. Thus, transaldolase or TPI activity does not influence the relative amounts of [1,2-$^{13}C_2$]- and [2,3-$^{13}C_2$]glucose, or the relative amount of [5,6-$^{13}C_2$]- and [4,5-$^{13}C_2$]glucose. If the PPP is not active (Fig. 1*C*), then the following (Equation 1) will occur regardless of transaldolase or disequilibrium at the level of TPI.

$$[1,2\text{-}^{13}C_2]/[2,3\text{-}^{13}C_2] = [5,6\text{-}^{13}C_2]/[4,5\text{-}^{13}C_2] \quad \text{(Eq. 1)}$$

Even if the PPP is active, ^{13}C in carbons 4–6 of glucose are not rearranged. However, the predominant isotopomers in the top half of glucose ([1,2,3-$^{13}C_3$]- and [2,3-$^{13}C_2$]glucose) will both be converted to [1,2-$^{13}C_2$]glucose. Therefore, if the PPP is active, then the following (Equation 2) will occur regardless of transaldolase or TPI activity.

$$[1,2\text{-}^{13}C_2]/[2,3\text{-}^{13}C_2] > [5,6\text{-}^{13}C_2]/[4,5\text{-}^{13}C_2] \quad \text{(Eq. 2)}$$

Contribution of PPP versus the CAC to Production of [1,2-$^{13}C_2$]glucose from [U-$^{13}C_3$]glycerol in Liver—Under the current experimental conditions, three glucose isotopomers in the top

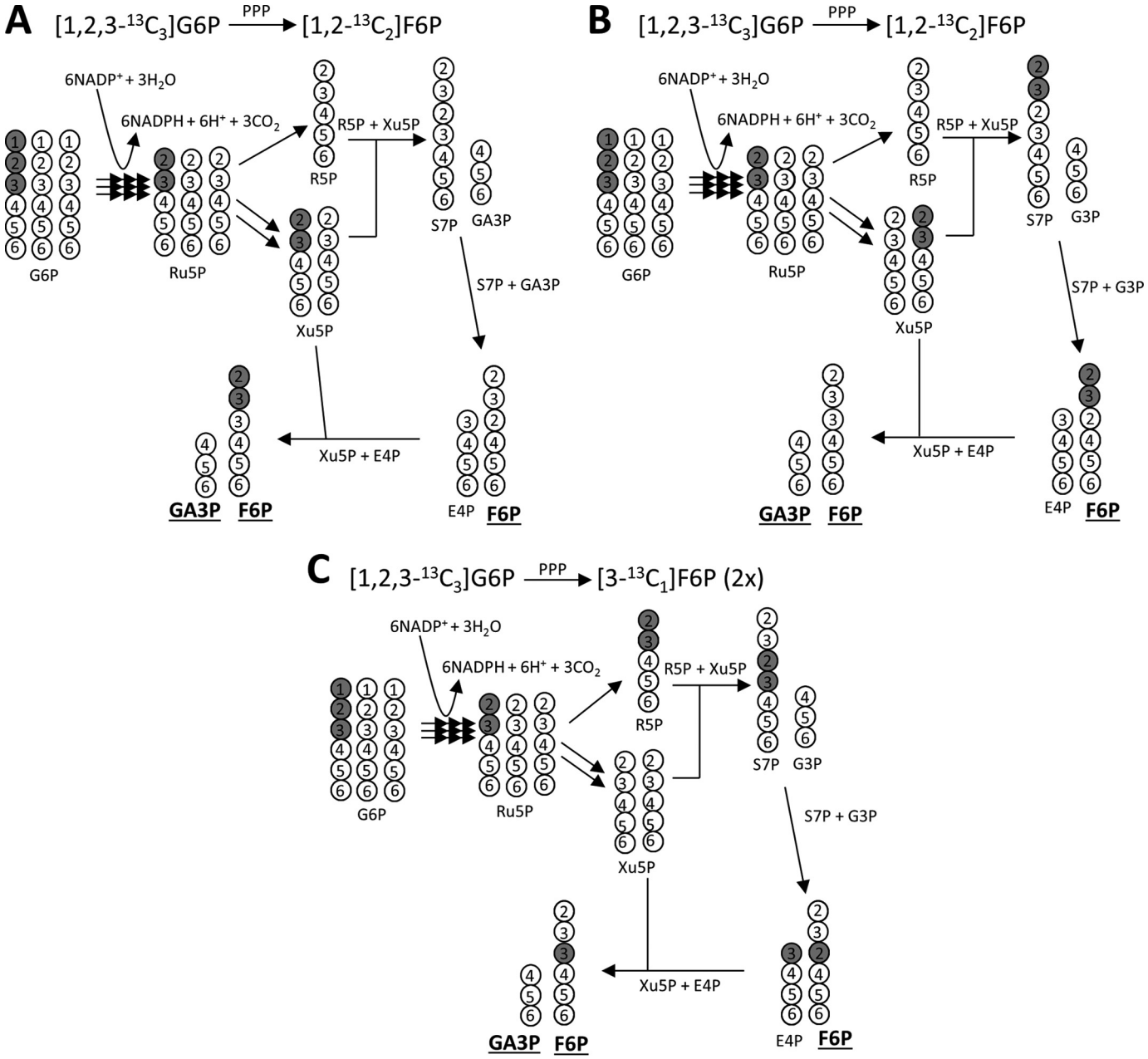

FIGURE 3. **[1,2-$^{13}C_2$]F6P Formation from [1,2,3-$^{13}C_3$]G6P through the pentose phosphate pathway.** The carbon 1 of G6P is decarboxylated in the oxidative phase of the PPP producing Ru5P; these carbons are further rearranged in the non-oxidative phase. The entry of three G6P molecules into the pentose pathway produces two F6P molecules and one GA3P molecule. If [1,2,3-$^{13}C_3$]G6P enters the pathway with unlabeled two G6P molecules, [1,2-$^{13}C_2$]F6P is formed through the routes illustrated in *A* or *B*. [3-$^{13}C_1$]F6P can be also produced through alternative pathways (*C*). The singly labeled hexose is not considered in this study to avoid complexity associated with natural abundance. Note that the order in carbons 4–6 of G6P remains the same through the PPP. All carbon numbers in this figure indicate the original carbon positions of G6P before the entry into the PPP. Metabolites *underlined* (F6P and GA3P) are the products after the PPP. *Ru5P*, ribulose 5-phosphate; *R5P*, ribose 5-phosphate; *Xu5P*, xylulose 5-phosphate; *open circle*, ^{12}C; *gray circle*, ^{13}C.

half of the molecule are derived from [U-$^{13}C_3$]glycerol: [1,2-$^{13}C_2$]-, [2,3-$^{13}C_2$]-, and [1,2,3-$^{13}C_3$]glucose. Similarly, other three isotopomers in the bottom half of the molecule are derived from [U-$^{13}C_3$]glycerol: [5,6-$^{13}C_2$]-, [4,5-$^{13}C_2$]-, and [4,5,6-$^{13}C_3$]glucose (Figs. 4 and 5). The fraction of plasma glucose derived from [U-$^{13}C_3$]glycerol was determined by measuring the total area of each distinct multiplet, referenced to the natural abundance ^{13}C signals in the methyl groups of MAG (21). Correction for T1 differences and nuclear Overhauser effects were negligible. The fraction of glucose derived from [U-$^{13}C_3$]glycerol via all pathways, including direct gluconeogenesis, entry into the CAC, the transaldolase reaction, and the PPP could be derived from a single ^{13}C NMR spectrum of plasma glucose (MAG).

Regardless of transaldolase activity, metabolism in the CAC, and incomplete equilibration by TPI, the ratio [1,2-$^{13}C_2$]/[2,3-$^{13}C_2$] must equal [5,6-$^{13}C_2$]/[4,5-$^{13}C_2$] in glucose unless the PPP is active. The entry of [1,2,3-$^{13}C_3$]glucose or [2,3-$^{13}C_2$]glucose through the PPP is the only mechanism to cause an increase of [1,2-^{13}C]glucose relative to [5,6-^{13}C]glucose, which increases the ratio of [1,2-^{13}C]/[2,3-$^{13}C_2$] relative to [5,6-^{13}C]/[4,5-$^{13}C_2$] in glucose after administration of [U-$^{13}C_3$]-

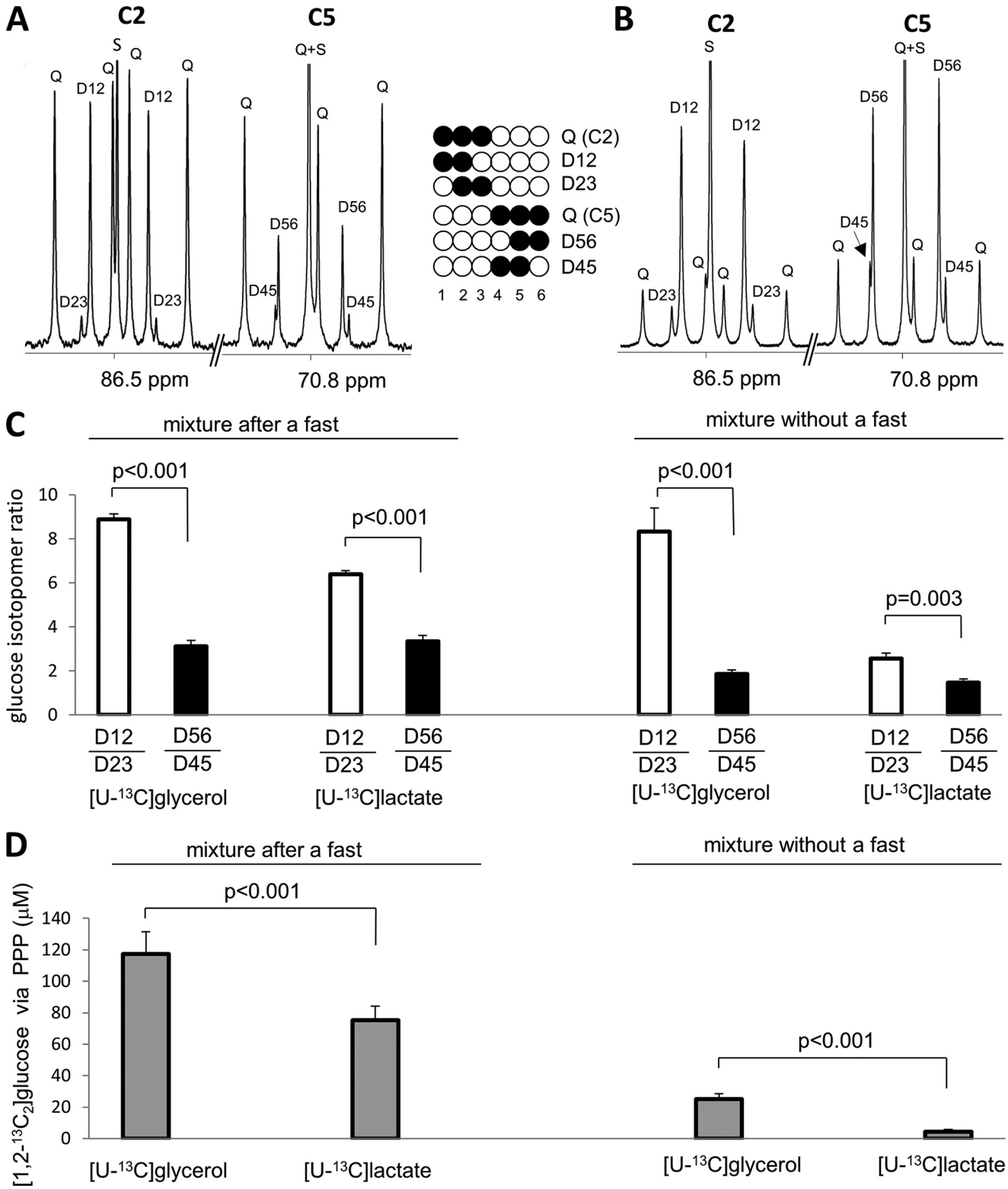

FIGURE 4. **Assessment of hepatic PPP activity based on NMR analysis of glucose using [U-$^{13}C_3$]glycerol *versus* [U-$^{13}C_3$]lactate.** Rats received a mixture of glucose, [U-$^{13}C_3$]glycerol, and lactate or a mixture of glucose, glycerol, and [U-$^{13}C_3$]lactate after a fast or without a fast. *A* shows ^{13}C NMR spectrum of MAG derived from blood glucose of a fasted rat given the mixture with [U-$^{13}C_3$]glycerol, whereas *B* shows that of a fasted rat given the mixture with [U-$^{13}C_3$]lactate. Rats given [U-$^{13}C_3$]glycerol had large differences in the ratios of [1,2-$^{13}C_2$]/[2,3-$^{13}C_2$] and [5,6-$^{13}C_2$]/[4,5-$^{13}C_2$] in glucose. Although these differences were present in rats given [U-$^{13}C_3$]lactate, the effect was less substantial, demonstrating the advantage of [U-$^{13}C_3$]glycerol over [U-$^{13}C_3$]lactate in the estimation of hepatic PPP activity (*C*). Consequently, rats given [U-$^{13}C_3$]glycerol had more [1,2-$^{13}C_2$]glucose in blood produced by the hepatic PPP activity compared with rats given [U-$^{13}C_3$]lactate (*D*). *D12*, doublet from coupling of C1 with C2; *D23*, doublet from coupling of C2 with C3; *Q*, doublet of doublets, or quartet, arising from coupling of C2 with both C1 and C3 or from coupling of C5 with both C4 and C6; *D45*, doublet from coupling of C4 with C5; *D56*, doublet from coupling of C5 with C6; *S*, singlet (n = 5–7 in each group).

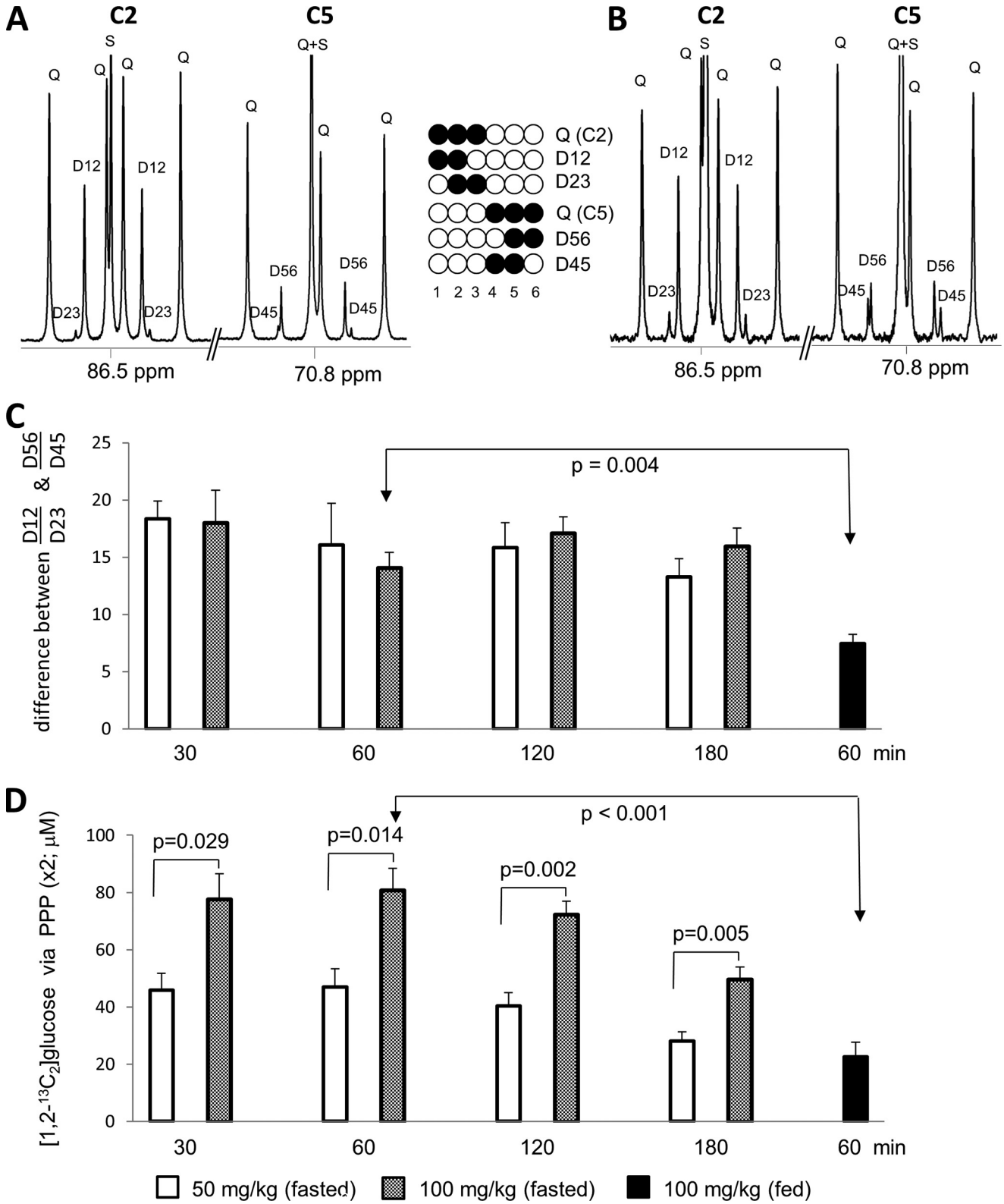

FIGURE 5. **Effects of dose and duration of [U-$^{13}C_3$]glycerol administration.** *A* and *B* show ^{13}C NMR spectra of MAG from blood glucose of a fasted (*A*) or fed (*B*) rat, and both rats received 100 mg/kg of [U-$^{13}C_3$]glycerol (50%), and blood was drawn at 60 min after the glycerol administration. In fasted rats, the ratio difference between [1,2-$^{13}C_2$]/[2,3-$^{13}C_2$] and [5,6-$^{13}C_2$]/[4,5-$^{13}C_2$] in glucose remained the same statistically over 180 min duration whether they received 50 or 100 mg/kg [U-$^{13}C_3$]glycerol (50%). However, fasted rats had higher ratio difference than fed animals when both groups received the same dose and duration of [U-$^{13}C_3$]glycerol administration (*i.e.* 100 mg/kg and 60 min; $p = 0.004$; *C*). The level of [1,2-$^{13}C_2$]glucose produced through the hepatic PPP (×2 due to 50% tracer) was higher in rats with 100 mg/kg [U-$^{13}C_3$]glycerol (50%) compared with rats with 50 mg/kg. Fasted rats had more [1,2-$^{13}C_2$]glucose produced by the PPP than fed animals (*D*) ($n = 4–6$ in each group).

glycerol. Consequently, $D12_{CAC}$ = D23·D56/D45 where $D12_{CAC}$ refers to the area of the D12 signal arising due to metabolism in the CAC, and the observed total area of $D12_{total} = D12_{CAC} + D12_{PPP}$. Thus, [1,2-$^{13}C_2$]glucose arising from PPP was determined by difference ($D12_{total} - D12_{CAC}$). The level of [1,2-$^{13}C_2$]glucose in blood produced through the PPP was calculated by multiplying the fraction of $D12_{PPP}$ and the [glucose].

As an example, the spectrum in Fig. 4*A* is from a rat with 9.6 mM plasma glucose. The fraction of plasma glucose derived from [U-$^{13}C_3$]glycerol was 16%. The ratio of $D12_{total}$/D23 was 9.1, whereas the ratio of D56/D45 was 3.8. Because $D12_{CAC}$/D23 = D56/D45, the peak area of $D12_{PPP}$ was obtained by subtracting $D12_{CAC}$ from $D12_{total}$. $D12_{PPP}$ represents [1,2-$^{13}C_2$]glucose produced only through the PPP, and it was 1.3% of plasma glucose in this animal. Thus, the level of [1,2-$^{13}C_2$]glucose in plasma produced from the PPP was 125 μM (= 9600 μM × 0.013).

Statistics—Data are expressed as means ± S.E. Comparisons between two groups were made using a Student's *t* test, where $p < 0.05$ was considered significant.

RESULTS

^{13}C-Labeling Patterns in Glucose Carbons 1–3 versus 4–6 with [U-$^{13}C_3$]Glycerol or [U-$^{13}C_3$]Lactate—The ^{13}C NMR spectrum of MAG derived from glucose in fasted rats given [U-$^{13}C_3$]glycerol, unlabeled glucose, and unlabeled lactate showed strong signals from both [1,2,3-$^{13}C_3$]glucose and [4,5,6-$^{13}C_3$]glucose as anticipated (Fig. 4*A*). This is consistent with high TPI activity. However, the pattern of ^{13}C labeling within carbons 1–3 compared with carbons 4–6 of glucose was quite different. The ratio [1,2-$^{13}C_2$]/[2,3-$^{13}C_2$] was dramatically higher compared with [5,6-$^{13}C_2$]/[4,5-$^{13}C_2$] in glucose (8.9 ± 0.3 *versus* 3.1 ± 0.2; $p < 0.001$; Fig. 4*C*). The difference (5.8 ± 0.2) was due to the PPP activity; it cannot arise from metabolism in the CAC, transaldolase, incomplete equilibration at TPI, or any combination of the pathways. When the label was provided in lactate rather than glycerol, the difference between [1,2-$^{13}C_2$]/[2,3-$^{13}C_2$] and [5,6-$^{13}C_2$]/[4,5-$^{13}C_2$] was smaller, only 3.1 ± 0.4 (Fig. 4, *B* and *C*).

^{13}C enrichment in plasma glucose was measured by the sum of all glucose isotopomers with excess ^{13}C, including singly-labeled glucose plus multiply labeled glucose such as [1,2-$^{13}C_2$]-, [2,3-$^{13}C_2$]-, [1,2,3-$^{13}C_3$]-, [5,6-$^{13}C_2$]-, [4,5-$^{13}C_2$]-, [4,5,6-$^{13}C_3$]-, and [U-$^{13}C_6$]glucose. In fasted rats supplied with [U-$^{13}C_3$]glycerol, unlabeled glucose, and unlabeled lactate, the sum of excess-labeled glucose isotopomers was 14.1 ± 1.6% whereas the sum in rats given [U-$^{13}C_3$]lactate, unlabeled glucose, and unlabeled glycerol was 11.8 ± 0.4%. In fasted rats given [U-$^{13}C_3$]glycerol, unlabeled glucose, and lactate, the fraction of [1,2-$^{13}C_2$]glucose produced through the hepatic PPP of all excess-labeled glucose isotopomers (PPP/gluconeogenesis from [U-$^{13}C_3$]glycerol) was 8.7 ± 0.3%. The fraction of plasma glucose derived from [U-$^{13}C_3$]glycerol after passage through the PPP was 1.23 ± 0.15%. In rats given [U-$^{13}C_3$]lactate, unlabeled glucose, and glycerol, the fraction (PPP/gluconeogenesis from [U-$^{13}C_3$]lactate) was 6.6 ± 0.7% and the fraction out of plasma glucose was 0.78 ± 0.09%. Consequently the amount of [1,2,-$^{13}C_2$]glucose in plasma produced through the PPP was higher in rats given [U-$^{13}C_3$]glycerol compared with rats given [U-$^{13}C_3$]lactate (118 ± 14 μM *versus* 75 ± 9 μM, $p < 0.001$; Fig. 4*D*). This difference arises because lactate must pass through the citric acid cycle and thus lose ^{13}C, prior to entry into gluconeogenesis.

Similar analysis was performed with NMR spectra from fed animals given [U-$^{13}C_3$]glycerol, unlabeled glucose, and unlabeled lactate or [U-$^{13}C_3$]lactate, unlabeled glucose, and unlabeled glycerol (supplemental Fig. 1 and Fig. 4, *C* and *D*). In the fed rats with [U-$^{13}C_3$]glycerol, the enrichment of [1,2,3-$^{13}C_3$]-glucose tended to be lower than that of [4,5,6-$^{13}C_3$]glucose without a statistically significant difference (0.78 ± 0.14% *versus* 1.16 ± 0.20%; $p = 0.146$). Selective labeling in carbons 4–6 of glucose is presumably due to both PPP and transaldolase reaction. However, again in fed rats given [U-$^{13}C_3$]glycerol, the [1,2-$^{13}C_2$]/[2,3-$^{13}C_2$] ratio was much higher compared with the [5,6-$^{13}C_2$]/[4,5-$^{13}C_2$] ratio (8.3 ± 1.1 *versus* 1.8 ± 0.2, $p <$ 0.001). Among fed rats given [U-$^{13}C_3$]lactate, unlabeled glucose, and unlabeled glycerol, the [1,2-$^{13}C_2$]/[2,3-$^{13}C_2$] ratio was only slightly higher than the [5,6-$^{13}C_2$]/[4,5-$^{13}C_2$] ratio (2.6 ± 0.3% *versus* 1.5 ± 0.2%; $p = 0.003$; Fig. 4*C*).

In fed rats given [U-$^{13}C_3$]glycerol, unlabeled glucose, and lactate, the fraction of [1,2-$^{13}C_2$]glucose produced by the PPP out of all excess-labeled glucose isotopomers (PPP/gluconeogenesis from [U-$^{13}C_3$]glycerol) was 8.4 ± 0.5%, and the fraction out of plasma glucose was 0.29 ± 0.04%. In fed rats given [U-$^{13}C_3$]lactate, unlabeled glucose, and unlabeled glycerol, the fraction (PPP/gluconeogenesis from [U-$^{13}C_3$]lactate) was 2.9 ± 0.5%, and the fraction out of plasma glucose was 0.05 ± 0.02%. Thus [1,2,-$^{13}C_2$]glucose produced by the PPP was 25.0 ± 3.4 μM in blood of fed rats given [U-$^{13}C_3$]glycerol and only 4.4 ± 1.3 μM in fed rats given [U-$^{13}C_3$]lactate (Fig. 4*D*).

The Effects of Dose and Duration of [U-$^{13}C_3$]Glycerol—^{13}C-Labeling patterns in blood glucose were examined in fasted rats given [U-$^{13}C_3$]glycerol (50%) only with different doses (25, 50, 100, or 500 mg/kg) and duration (30, 60, 120, or 180 min). The unique labeling pattern produced by the hepatic PPP activity in glucose (*i.e.* [1,2-$^{13}C_2$]/[2,3-$^{13}C_2$] > [5,6-$^{13}C_2$]/[4,5-$^{13}C_2$]) was observed in all animals given 50%[U-$^{13}C_3$]glycerol, regardless of the glycerol dose or interval between administration and blood sampling. Typical spectra are shown in Fig. 5, *A* and *B*. After glycerol administration, plasma glucose levels remained the same with lower doses up to 100 mg/kg, but increased with 500 mg/kg dose (Table 1). The dose of 25 mg/kg [U-$^{13}C_3$]glycerol (50%) resulted in ~1–3% glucose isotopomers in blood, and 500 mg/kg resulted in ~20–30% (Table 1). The lowest dose and the highest dose were not further considered in the current work due to some difficulties in NMR spectral analysis. The low enrichment caused low signal-to-noise ratio in the ^{13}C NMR spectra, whereas the high enrichment is associated with long range ^{13}C-^{13}C spin-spin couplings in MAG derived from [U-$^{13}C_6$]glucose and other isotopomers labeled in the top and bottom half of glucose. Both low S/N resulting from low enrichment and long range couplings resulting from high enrichment complicated the analysis of the NMR data. Doses with 50 mg/kg and 100 mg/kg resulted in ~2–6% and ~4–10%, respectively, providing reasonable enrichments for accurate analysis.

TABLE 1

The effects of dose and duration of [U-$^{13}C_3$]glycerol on plasma glucose

Rats received different doses of [U-$^{13}C_3$]glycerol (50%), and blood was collected at different time points.

Dose (mg/kg)	0 (fasted) (n = 4)	25 (fasted) (n = 1)	50 (fasted) (n = 4–5)	100 (fasted) (n = 5–8)	500 (fasted) (n = 1)	100 (fed) (n = 5)
Plasma glucose (mmol/liter)						
30 min	–	6.6	7.1 ± 0.5	7.1 ± 0.3	9.9[a]	–
60 min	6.3 ± 0.4	7.1	6.7 ± 0.2	6.7 ± 0.3	9.1	8.8 ± 0.3[a]
120 min	–	6.8	6.9 ± 0.5	6.1 ± 0.2	7.7	–
180 min	–	6.5	6.7 ± 0.4	5.7 ± 0.3	7.4	–
Isotopomer enrichment in plasma glucose (%)[b]						
30 min	–	2.6	6.4 ± 0.5	9.7 ± 0.8	29.4	–
60 min	–	2.8	5.2 ± 0.0	9.9 ± 0.6	32.5	2.1 ± 0.3
120 min	–	1.5	3.1 ± 0.4	6.5 ± 0.4	28.4	–
180 min	–	1.1	2.2 ± 0.3	4.5 ± 0.3	18.4	–
Plasma glucose derived from the PPP (%)[c]						
30 min	–	–	0.62 ± 0.05	1.05 ± 0.10	–	–
60 min	–	–	0.70 ± 0.09	1.21 ± 0.07	–	0.26 ± 0.06
120 min	–	–	0.56 ± 0.07	1.17 ± 0.08	–	–
180 min	–	–	0.42 ± 0.03	0.87 ± 0.06	–	–
PPP/glycerol gluconeogenesis (%)[d]						
30 min	–	–	5.7 ± 0.2	5.5 ± 0.2	–	–
60 min	–	–	6.6 ± 0.9	6.3 ± 0.5	–	6.2 ± 0.9
120 min	–	–	9.1 ± 0.6	8.7 ± 0.6	–	–
180 min	–	–	9.8 ± 1.0	9.8 ± 0.5	–	–

[a] Compared to the fasted rats with 0 mg/kg (60 min), the fasted rat with 500 mg/kg (30 min) had higher plasma glucose (p = 0.036), and the fasted rat with 500 mg/kg (60 min) tended to have higher glucose (p = 0.066). The fed rats with 100 mg/kg (60 min) also had higher plasma glucose levels compared to the fasted rats with 0 mg/kg (60 min) (p = 0.002) or compared with the fasted rats with 100 mg/kg (60 min) ($p < 0.001$).

[b] The enrichment is the sum of all the glucose isotopomers with excess ^{13}C in blood of rats given 50% [U-$^{13}C_3$]glycerol.

[c] Due to 50% labeled tracer, the number in this subset is the doubled value of the enrichment of [1,2-$^{13}C_2$]glucose produced from the hepatic PPP activity.

[d] The value is the percentage of [1,2-$^{13}C_2$]glucose produced by the hepatic PPP of all glucose isotopomers with excess ^{13}C produced through gluconeogenesis from [U-$^{13}C_3$]glycerol.

The ratio difference of glucose isotopomers ([1,2-$^{13}C_2$]/[2,3-$^{13}C_2$] *versus* [5,6-$^{13}C_2$]/[4,5-$^{13}C_2$]) in the fasted rats remained essentially the same statistically from 30 to 180 min, whether they received 50 or 100 mg/kg [U-$^{13}C_3$]glycerol (Fig. 5*C*). The level of glucose derived from the exogenous glycerol was ~0.4–0.8% (2× enrichment of $D12_{ppp}$) of plasma glucose with 50 mg/kg [U-$^{13}C_3$]glycerol (50%) and ~0.9–1.3% with 100 mg/kg in fasted rats (Table 1). Thus, [1,2-$^{13}C_2$]glucose produced by the hepatic PPP was higher in rats with 100 mg/kg (Fig. 5*D*). The percentage of [1,2-$^{13}C_2$]glucose produced by the PPP of all excess labeled glucose isotopomers was ~5–10%, and it was increased with time (Table 1).

The Effect of Feeding on ^{13}C-Labeling Patterns in Glucose Carbons 1–3 versus 4–6—^{13}C-Labeling pattern in glucose was compared between fed and fasted animals, which both had received 100 mg/kg [U-$^{13}C_3$]glycerol (50%) and collected blood after 60 min. Compared with fasted animals, fed animals had lower excess ^{13}C-labeled glucose isotopomers, the ratio difference ([1,2-$^{13}C_2$]/[2,3-$^{13}C_2$] *versus* [5,6-$^{13}C_2$]/[4,5-$^{13}C_2$]), and the amount of [1,2-$^{13}C_2$]glucose produced by the PPP, but the ratio of PPP/gluconeogenesis from [U-$^{13}C_3$]glycerol was the same (Fig. 5 and Table 1).

DISCUSSION

This study presents a novel method to estimate the hepatic PPP activity in animals based on the ^{13}C-labeling pattern of blood glucose after [U-$^{13}C_3$]glycerol administration. In the presence of [U-$^{13}C_3$]glycerol, numerous labeling patterns in glucose can arise as a consequence of glycerol metabolism in the CAC prior to gluconeogenesis, the transaldolase reaction, incomplete equilibration in the triose pool, and flux through the PPP. Only one of these four pathways, flux through the PPP, can alter the distribution of ^{13}C doubly labeled isotopomers within the top half of glucose compared with the bottom half. The PPP activity was determined by ^{13}C NMR analysis of excess [1,2-$^{13}C_2$]/[2,3-$^{13}C_2$] compared with [5,6-$^{13}C_2$]/[4,5-$^{13}C_2$] in glucose. The altered labeling pattern due to the PPP activity was observed in all the animals given [U-$^{13}C_3$]glycerol whether they were fed or fasted. To our knowledge, this is the first report of detection of hepatic PPP activity *in vivo* using a stable isotope tracer.

In contrast to [U-$^{13}C_3$]lactate, the use of [U-$^{13}C_3$]glycerol resulted in dramatic ^{13}C asymmetry in blood glucose through the interaction between hepatic PPP and gluconeogenesis from [U-$^{13}C_3$]glycerol. Although the PPP activity was small, less than ~10% of gluconeogenesis from [U-$^{13}C_3$]glycerol, the altered ^{13}C-labeling patterns induced by the PPP are easily detected using [U-$^{13}C_3$]glycerol as the tracer. In contrast, the use of [U-$^{13}C_3$]lactate instead of [U-$^{13}C_3$]glycerol yielded only minor difference in the ^{13}C-labeling pattern in glucose produced by livers presumably with identical PPP activities. This demonstrates the importance of selecting the proper substrate for sensitivity in the estimation of hepatic PPP activity. Among the many possible gluconeogenic tracers, [U-$^{13}C_3$]glycerol is uniquely suited to detecting the PPP because it is incorporated, largely intact, in gluconeogenesis at the level of trioses. Consequently, glucose derived from [U-$^{13}C_3$]glycerol is relatively highly enriched. Other common gluconeogenic tracers such as ^{13}C-labeled lactate, alanine, or pyruvate undergo obligatory metabolism in the CAC where the ^{13}C label is substantially diluted, which makes these labeled molecules much less efficient for the detection of hepatic PPP activity.

After [U-$^{13}C_3$]glycerol administration, [5,6-$^{13}C_2$]glucose and [4,5-$^{13}C_2$]glucose can only arise from metabolism in the CAC and not as a consequence of the PPP. The ^{13}C labeling in car-

bons 4–6 of glucose was used to measure the excess [1,2-$^{13}C_2$]glucose relative to [2,3-$^{13}C_2$]glucose, which can be attributed to PPP activity. The primary activity that causes the difference in the ratios is the entry of [1,2,3-$^{13}C_3$]hexose into the PPP producing [1,2-$^{13}C_2$]hexose. Thus, the method presented here detects only the lower limit of PPP activity because not all [1,2,3-$^{13}C_3$]hexose entering the PPP cycle results in [1,2-$^{13}C_2$]hexose. Based on the data from rats given 50 or 100 mg/kg [U-$^{13}C_3$]glycerol (50%), the ratio difference between [1,2-$^{13}C_2$]/[2,3-$^{13}C_2$] and [5,6-$^{13}C_2$]/[4,5-$^{13}C_2$] in glucose remained essentially the same regardless of the dose or the duration up to 180 min after tracer administration. However, the level of [1,2-$^{13}C_2$]glucose in plasma produced by the PPP was subject to the dose and to the interval between administration and blood sampling. In addition, nutritional states affected both the ratio difference and the amount of [1,2-$^{13}C_2$]glucose derived by the PPP. Thus, the method presented in the current study should be performed under the same conditions in tracer selection, dose, timing, and nutritional state between a study group and control.

In the study with rats given only glycerol without other substrates, 50% labeled glycerol was chosen to minimize the appearance of long range couplings of MAG derived essentially from [U-$^{13}C_6$]glucose. [U-$^{13}C_6$]Glucose is formed by condensing two [U-$^{13}C_3$]trioses, which generate significant signal in glucose from fasted animals given pure [U-$^{13}C_3$]glycerol (spectra not shown). The formation of [U-$^{13}C_6$]glucose was reduced by using 50%[U-$^{13}C_3$]glycerol instead of 100%. Long range couplings were minor in animals given 100%[U-$^{13}C_3$]glycerol plus unlabeled glucose and lactate. However, a high dose (*i.e.* 500 mg/kg) of 50%[U-$^{13}C_3$]glycerol still produced some [U-$^{13}C_6$]-glucose that might affect the accuracy in spectral analysis, which was not further studied in the current work.

Stable isotopes have not been used previously for measurement of hepatic PPP activity *in vivo*, and there are few studies using radiotracers. Magnusson *et al.* (20) used two radioactive tracers simultaneously, [1-$^{14}C_1$]ribose and [2-$^{14}C_1$]glucose, in human subjects. The ^{14}C from the both tracers was found in the carbon 1 or 3 position of hexoses as a consequence of the PPP (see Fig. 3). In that study, glucuronides excreted in urine after diflunisal and acetaminophen administration were analyzed. The current approach differs substantially in several respects. First, the use of radiotracers in human patient studies is limiting. Second, blood was sampled from the hepatic vein, an invasive procedure requiring further ionizing radiation because of the use of fluoroscopy to confirm that urinary glucuronides reliably reported ^{14}C in hepatic glucose. Analysis of glucuronides requires administration of drugs such as acetaminophen. Because many drugs are detoxified in the liver, drug administration itself may potentially alter the hepatic PPP activity. The current method is essentially non-invasive as blood sampling can be done from any venous vessels with easy access, which is possible because the liver is the dominant gluconeogenic organ in the body.

In the settings of isolated livers or cell cultures, the PPP was measured typically with ^{13}C- or ^{14}C-labeled glucose tracers based on the loss of glucose carbon 1 in the oxidative phase. For instance, the participation of [1,2-$^{13}C_2$]glucose (or [1,2-$^{13}C_2$]G6P) in the PPP produces [1-$^{13}C_1$]F6P and consequently [3-$^{13}C_1$]lactate plus unlabeled lactate through glycolytic process. In contrast, glycolysis of [1,2-$^{13}C_2$]glucose without the PPP interruption produces [2,3-$^{13}C_2$]lactate plus unlabeled lactate. Thus, excess [3-$^{13}C_1$]lactate reflects the activity of the PPP. In another case, both [1-$^{13}C_1$]glucose and [6-$^{13}C_1$]glucose are used together, and only [1-$^{13}C_1$]glucose loses ^{13}C through the PPP, whereas [6-$^{13}C_1$]glucose does not. These approaches are feasible in isolated organs or cell cultures but cannot be applied *in vivo* for the detection of hepatic PPP activity because other organs in the body also utilize glucose. In principle, blood can be drawn from hepatic vein as discussed above, but it is invasive.

In summary, the hepatic PPP activity in live rats was estimated by analyzing ^{13}C-labeling patterns in blood glucose after [U-$^{13}C_3$]glycerol administration. This approach is readily applicable in any clinical setting as it only requires ingestion of [U-$^{13}C_3$]glycerol and a simple blood draw followed by glucose analysis using ^{13}C NMR. The hepatic PPP activity is particularly of interest in part because of its roles for antioxidant defense and abnormal cell growth. NADPH and ribose are the major products from the PPP, which are essential in the replenishment of reduced glutathione and in nucleotide synthesis, respectively.

Acknowledgments—We thank Nicholas Carpenter, Xiaodong Wen, Charles Storey, and Angela Milde for excellent technical support.

REFERENCES

1. Guo, Z. K., Lee, W. N., Katz, J., and Bergner, A. E. (1992) Quantitation of positional isomers of deuterium-labeled glucose by gas chromatography/mass spectrometry. *Anal. Biochem.* **204,** 273–282
2. Katz, J., Wals, P., and Lee, W. N. (1993) Isotopomer studies of gluconeogenesis and the Krebs cycle with ^{13}C-labeled lactate. *J. Biol. Chem.* **268,** 25509–25521
3. Landau, B. R., Wahren, J., Chandramouli, V., Schumann, W. C., Ekberg, K., and Kalhan, S. C. (1996) Contributions of gluconeogenesis to glucose production in the fasted state. *J. Clin. Invest.* **98,** 378–385
4. Schumann, W. C., Magnusson, I., Chandramouli, V., Kumaran, K., Wahren, J., and Landau, B. R. (1991) Metabolism of [2-^{14}C]acetate and its use in assessing hepatic Krebs cycle activity and gluconeogenesis. *J. Biol. Chem.* **266,** 6985–6990
5. Neese, R. A., Schwarz, J. M., Faix, D., Turner, S., Letscher, A., Vu, D., and Hellerstein, M. K. (1995) Gluconeogenesis and intrahepatic triose phosphate flux in response to fasting or substrate loads: application of the mass isotopomer distribution analysis technique with testing of assumptions and potential problems. *J. Biol. Chem.* **270,** 14452–14466
6. Veech, R. L., Raijman, L., Dalziel, K., and Krebs, H. A. (1969) Disequilibrium in the triose phosphate isomerase system in rat liver. *Biochem. J.* **115,** 837–842
7. Hostetler, K. Y., Williams, H. R., Shreeve, W. W., and Landau, B. R. (1969) Conversion of specifically ^{14}C-labeled lactate and pyruvate to glucose in man. *J. Biol. Chem.* **244,** 2075–2077
8. Magnusson, I., Schumann, W. C., Bartsch, G. E., Chandramouli, V., Kumaran, K., Wahren, J., and Landau, B. R. (1991) Noninvasive tracing of Krebs cycle metabolism in liver. *J. Biol. Chem.* **266,** 6975–6984
9. Previs, S. F., Hallowell, P. T., Neimanis, K. D., David, F., and Brunengraber, H. (1998) Limitations of the mass isotopomer distribution analysis of glucose to study gluconeogenesis. Heterogeneity of glucose labeling in incubated hepatocytes. *J. Biol. Chem.* **273,** 16853–16859
10. Previs, S. F., Fernandez, C. A., Yang, D., Soloviev, M. V., David, F., and Brunengraber, H. (1995) Limitations of the mass isotopomer distribution analysis of glucose to study gluconeogenesis. Substrate cycling between glycerol and triose phosphates in liver. *J. Biol. Chem.* **270,** 19806–19815

11. Jin, E. S., Sherry, A. D., and Malloy, C. R. (2013) Metabolism of glycerol, glucose and lactate in the citric acid cycle prior to incorporation into hepatic acylglycerols. *J. Biol. Chem.* **288,** 14488–14496
12. Bock, G., Schumann, W. C., Basu, R., Burgess, S. C., Yan, Z., Chandramouli, V., Rizza, R. A., and Landau, B. R. (2008) Evidence that processes other than gluconeogenesis may influence the ratio of deuterium on the fifth and third carbons of glucose: implications for the use of $^{2}H_{2}O$ to measure gluconeogenesis in humans. *Diabetes* **57,** 50–55
13. Inbar, L., and Lapidot, A. (1991) ^{13}C nuclear magnetic resonance and gas chromatography-mass spectrometry studies of carbon metabolism in the actinomycin D producer Streptomyces parvulus by use of ^{13}C-labeled precursors. *J. Bacteriol.* **173,** 7790–7801
14. Ljungdahl, L., Wood, H. G., Couri, D., and Racker, E. (1961) Formation of unequally labelled fructose-6-phosphate by an exchange reaction catalyzed by transaldolase. *J. Biol. Chem.* **236,** 1622–1625
15. Browning, J. D., and Burgess, S. C. (2012) Use of $^{2}H_{2}O$ for estimating rates of gluconeogenesis: determination and correction of error due to transaldolase exchange. *Am. J. Physiol. Endocrinol. Metab.* **303,** E1304–E1312
16. Jones, J. G., Garcia, P., Barosa, C., Delgado, T. C., Caldeira, M. M., and Diogo, L. (2008) Quantification of hepatic transaldolase exchange activity and its effects on tracer measurements of indirect pathway flux in humans. *Magn. Reson. Med.* **59,** 423–429
17. Jin, E. S., Sherry, A. D., and Malloy, C. R. (2013) Evidence for transaldolase activity in the isolated heart supplied with [U-$^{13}C_{3}$]glycerol. *J. Biol. Chem.* **288,** 2914–2922
18. Kurland, I. J., Alcivar, A., Bassilian, S., and Lee, W. N. (2000) Loss of [^{13}C]glycerol carbon via the pentose cycle. Implications for gluconeogenesis measurement by mass isotoper distribution analysis. *J. Biol. Chem.* **275,** 36787–36793
19. Landau, B. R., Bartsch, G. E., Katz, J., and Wood, H. G. (1964) Estimation of pathway contributions to glucose metabolism and of the rate of isomerization of hexose 6-phosphate. *J. Biol. Chem.* **239,** 686–696
20. Magnusson, I., Chandramouli, V., Schumann, W. C., Kumaran, K., Wahren, J., and Landau, B. R. (1988) Pentose pathway in human liver. *Proc. Natl. Acad. Sci. U.S.A.* **85,** 4682–4685
21. Jin, E. S., Jones, J. G., Merritt, M., Burgess, S. C., Malloy, C. R., and Sherry, A. D. (2004) Glucose production, gluconeogenesis, and hepatic tricarboxylic acid cycle fluxes measured by nuclear magnetic resonance analysis of a single glucose derivative. *Anal. Biochem.* **327,** 149–155